DOI: 10.1002/chem.200500111

Covalent Incorporation of Methyl Red Dyes into Double-Stranded DNA for Their Ordered Clustering

Hiromu Kashida,[a] Masayuki Tanaka,[a] Seiki Baba,[b] Taiichi Sakamoto,[b] Gota Kawai,[b] Hiroyuki Asanuma,*[a, c] and Makoto Komiyama[a]

Abstract: An ordered dye cluster of Methyl Reds was formed in double-stranded DNA by hybridizing two complementary DNA–dye conjugates, each involving a Methyl Red moiety on a threoninol linker and a 1,3-propanediol spacer arranged alternately in the middle of the DNA sequence. In the duplex, Methyl Reds from each strand were axially stacked antiparallel to each other, as determined from NMR analysis. This clustering of Methyl Reds induced distinct changes in both UV/Vis and CD spectra. Single-stranded DNA–Methyl Red conjugates on D-threoninol linkers and (1,3-propanediol) spacers exhibited broad absorption spectra with λ_{max} at around 480 nm, and almost no CD was observed at around the absorption maximum of Methyl Red. However, as Methyl Reds were clustered by hybridization, λ_{max} shifted towards shorter wavelengths with respect to its monomeric transition. This hypsochromic shift increased as the number of Methyl Red molecules increased. Furthermore, a positive couplet was also strongly induced here. These dye clusters are H-aggregates, in which molecular excitons are coupled. The positive couplet demonstrates that the clusters on D-threoninol form a right-handed helix. In contrast, the induced CD became much weaker with Methyl Red on L-threoninol, which intrinsically prefers counterclockwise winding. Thus, mutual orientation of the stacked dye molecules was controlled by the chirality of the linker.

Keywords: DNA recognition · DNA · dyes/pigments · NMR spectroscopy · UV/Vis spectroscopy

[a] H. Kashida, M. Tanaka, Prof. Dr. H. Asanuma, Prof. Dr. M. Komiyama
Research Center for Advanced Science and Technology
The University of Tokyo
Komaba, Meguro-ku, Tokyo 153-8904 (Japan)
E-mail: asanuma@mol.nagoya-u.ac.jp

[b] Dr. S. Baba, Dr. T. Sakamoto, Prof. Dr. G. Kawai
Department of Industrial Chemistry
Chiba Institute of Technology
2-17-1 Tsudanuma, Narashino-shi, Chiba 275-0016 (Japan)

[c] Prof. Dr. H. Asanuma
Precursory Research for Embryonic Science and Technology (PRESTO)
Japan Science and Technology Agency (JST)
Kawaguchi, Saitama 332-0012 (Japan)
Current address:
Department of Molecular Design and Engineering
Graduate School of Engineering, Nagoya University
Chikusa, Nagoya 464-8603 (Japan)
Fax: (+81) 52-789-2528

Supporting information for this article is available on the WWW under http://www.chemeurj.org/ or from the author: Table S1 (Statistical restraints for the structural determination), Figure S1 (Schematic representation of the electronic transitions), Figure S2 (NOESY at 50 °C), Figure S3 (Superimposition of the converged structures), Figure S4 (CD spectra of **DS*n*A**/**DS*n*B** at 300–200 nm), Figure S5 (Thermal change in UV/Vis and CD spectra of **DS3A**/**DS3B**), Figure S6 (Comparison of UV/Vis spectrum of the **DS3A**/**DS3B** duplex with that of **D6**), Figure S7 (Melting curves for **DS*n*A**/**DS*n*B** and **LS*n*A**/**LS*n*B**).

Introduction

Organized clusters of inorganic or organic molecules exhibit interesting properties that cannot be attained in their monomeric state.[1,2] Because their properties depend on the orientation and size of the assemblies, various methodologies for controlling the structure assembled from a desired number of molecules have been proposed (so called bottom-up nanotechnology).[3,4] Recently, poly- or oligodeoxyribonucleotide (DNA) has been applied for this purpose: intercalators or groove-binders that strongly interact with nucleotides can be aligned along the natural DNA duplex.[5] The covalent incorporation of these molecules into DNA can achieve the clustering of functional molecules, which is possible due to advances in phosphoramidite chemistry that have enabled the introduction of various molecules into DNA.[6] By programming the DNA sequence, a one-dimensional wire of metal complexes or dye assembly has been successfully prepared.[7] Thus, DNA is a convenient scaffold for creating a variety of new supramolecules.

Covalent incorporation of clustered functional molecules into double-stranded DNA is also advantageous in extending the potential applications of DNA. Recently, DNA has been highlighted not only in the fields of molecular biology and biotechnology, but also in the field of nanomaterial

chemistry.[8] Highly organized base-pairs that are aligned along the axis of the helix exhibit unexpectedly interesting properties, such as conductivity. Precise strand recognition makes it possible to construct various nanomachines,[9] DNA computers,[10] and nanowires.[11] However, because the four natural nucleic acid bases are not optimized for such applications, the introduction of other functional clusters into the double-stranded DNA may offer promising improvements in the properties exhibited.

Previously, we synthesized a one-dimensional Methyl Red cluster of desired size by incorporating Methyl Reds sequentially into the single-stranded DNA.[12] UV/Vis spectra of this cluster in the single strand exhibited a large hypsochromic shift and distinct narrowing of the band with respect to that of the monomeric Methyl Red.[13] In this cluster, the Methyl Reds are stacked parallel to each other, and thus, both the narrowing and hypsochromic shift of the band were observed, due to the strong exciton coupling among the dye molecules. However, this stable cluster forms only in the single-stranded state, not in the duplex. As this strand including the Methyl Red cluster was hybridized with a complementary DNA, hypsochromicity due to the strong exciton coupling disappeared, because the highly ordered cluster was destroyed. Therefore, this cluster design cannot be applied to the modification of double-stranded DNA.

Here, we report the design of another stable one-dimensional cluster of functional molecules that is formed in double-stranded DNA. This cluster is prepared from two complementary DNA conjugates, each of which involve a dye moiety and spacer residue arranged alternately in the middle of the DNA sequence, as shown in Scheme 1. At each end of each strand, natural nucleotides are attached as a tag. With the aid of these natural nucleotides, the two strands can be hybridized and, thus, the dye molecules are forced to assemble at the center of the double-stranded DNA, as illustrated in Scheme 1a. Here again, we use Methyl Red as a model dye because 1) the size of the dye fits the base-pair and 2) its asymmetric structure is suitable for demonstrating the effect of the relative orientation (parallel or antiparallel) of the dye on the optical properties.[14] By using Methyl Red, the interstrand clustering of the dye molecules based on this design is demonstrated, and both the stacked structure and the spectroscopic behavior are investigated in detail. We show that the dye moieties are stacked antiparallel to each other, as evidenced by NMR analysis. This cluster also exhibits distinct hypsochromicity, due to the exciton coupling (H-band), which is different from our previous parallel cluster of Methyl Reds in the single-stranded DNA.

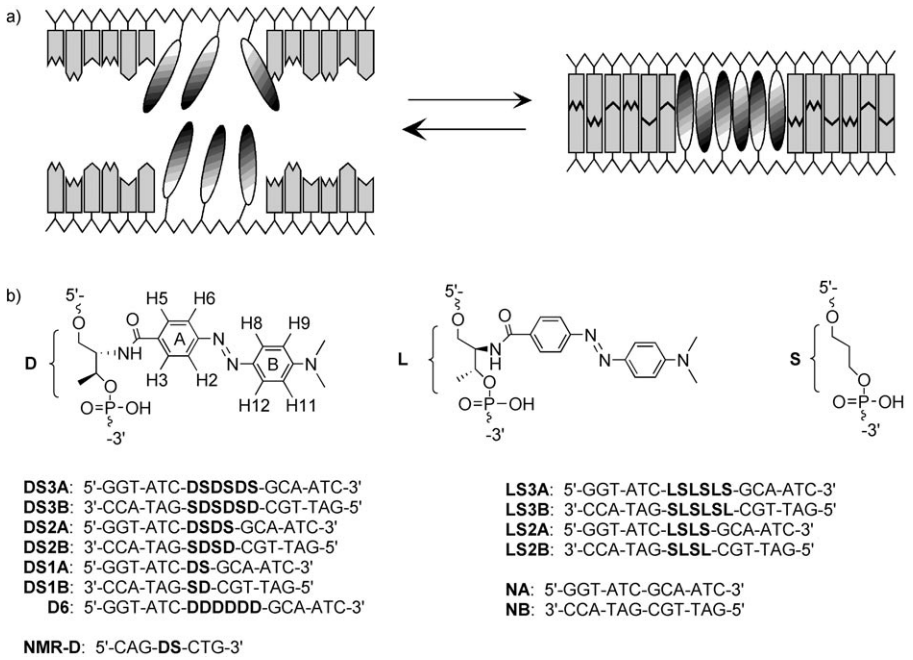

Scheme 1. a) Illustration of our design for the clustering of functional molecules. b) the DNA–Methyl Red conjugates synthesized in this study.

Results

Direct evidence for the stacking of Methyl Reds and structure determination by NMR analysis

*NOESY analysis of the **NMR-D** species*: Our design for the clustering of Methyl Reds is schematically illustrated in Scheme 1a. Methyl Red on D- or L-threoninol (**D** or **L** residues in Scheme 1b) and 1,3-propanediol (**S** in Scheme 1b) were alternately introduced at the center of the DNA sequence. Here, the **S** residue was located as the counterpart of the **D** or **L** residue, and Methyl Red moieties from both strands were stacked against each other by the tentative "base-pairing" between **D** (or **L**) and **S**. Leumann has reported interstrand clustering of bipyridyl C-nucleotide residues in the absence of **S** residues.[15] In our design, **S** residues were introduced to avoid the strong clustering of Methyl Reds in the single-stranded state.[12a,16] To verify the validity of this design for dye clustering, NMR analysis was conducted initially with a Methyl Red dimer formed from the self-complementary conjugate **NMR-D**, shown in Scheme 1b. Because the melting temperature of the **NMR-D** duplex was 26.0 °C,[17] NMR measurements were performed at 7 °C (280 K). The symmetry of **NMR-D** with eight

distinct units gives three unique natural base-pairs (C^1–G^{16}, A^2–T^{15}, and G^3–C^{14}, shown within the box in Figure 1) and one tentative **D**–**S** pair (D^4–S^{13}). One- and two-dimensional NMR spectra, measured in both H_2O (H_2O/D_2O 9:1) and

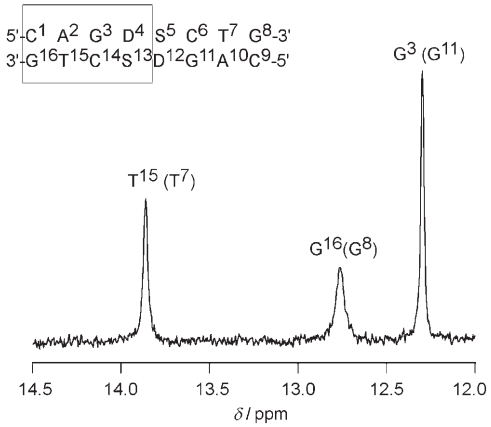

Figure 1. One-dimensional NMR spectrum of the **NMR-D** self-complementary duplex at the imino region in H_2O/D_2O 9:1 at 280 K (mixing time = 150 ms), pH 7.0 (10 mM phosphate buffer), in the presence of 200 mM NaCl. Concentration of **NMR-D** was 1.0 mM. Imino-proton assignments are denoted on the spectrum with the residue number shown at the top.

D_2O, provide structural information. These spectra combined with the NOESY, DQF-COSY, and TOCSY spectra obtained in D_2O allowed most of the signals of the duplex to be assigned. In Figure 1, the one-dimensional NMR spectrum measured in H_2O at the region of the imino-protons (12–14.5 ppm) is depicted. As expected, there were three individual signals that could be assigned on the basis of the NOESY and chemical shift of each signal, indicating that the non-natural **D** and **S** do not interfere with the base-pairing. The imino-proton signal of the terminal G^{16} was rather broad, due to the rapid exchange with water, whereas that of G^3 adjacent to the D^4 residue remained sharp.[18] Figure 2 depicts the NOEs between the imino-proton signal (12–14 ppm) and the aromatic-proton signal (5.5–7.5 ppm) regions. A distinct NOE signal was observed between the imino proton of G^3 and both H8 (H12) and H9 (H11) of the Methyl Red protons, indicating that the Methyl Red moiety is not flipped out, but is intercalated. Intercalation of Methyl Red is further confirmed from NOE between the protons on the dimethylamino group of Methyl Red and trimethylene protons on the **S** residue (data not shown).

Stacking of Methyl Reds was also evidenced from the NOESY data, as shown in Figure 3. NOE signals were observed between H11 (H9) and H3 (H5), and H11 (H9) and H2 (H6) (Figure 3a), indicating that two Methyl Reds were stacked in an antiparallel manner. Antiparallel stacking was further confirmed from the NOE between N-CH_3 and H2 (H6), and N-CH_3 and H3 (H5) (Figure 3b), because these NOEs were too large to originate from an intramolecular Methyl Red moiety. Consistently, these NOE signals disappeared as the temperature was elevated to 50 °C, which causes dissociation of the duplex.[19] All these NOEs demonstrate that Methyl Red molecules are stacked antiparallel to each other, as shown in Figure 3c, which validates our design for the clustering of the Methyl Reds.

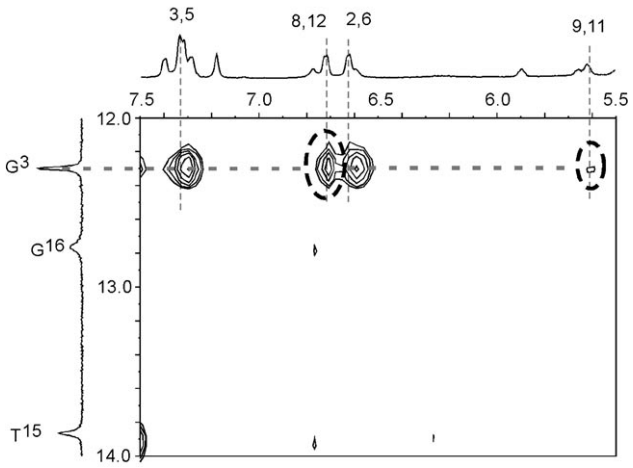

Figure 2. Two-dimensional NOESY spectrum (mixing time = 150 ms) between the aromatic-proton signal (5.5–7.5 ppm) and imino-proton signal regions (12–14 ppm) for the **NMR-D** duplex in H_2O/D_2O 9:1 at 280 K, pH 7.0 (10 mM phosphate buffer), in the presence of 200 mM NaCl. Assignments of azobenzene protons are denoted on the one-dimensional spectra (*F*2 axis) by the numbers designated in Scheme 1b. The NOE signals surrounded by broken circles demonstrate intercalation of Methyl Red.

Structure determination: The distances between all the atoms in the duplex were calculated according to the strength of NOE. A total of 256 NOE distance restraints were used for the calculation. The duplex structures were calculated by using restrained molecular dynamics of a simulated annealing protocol (see Experimental Section for details). A total of ten final structures converged to low total energy. The minimized averaged structure is shown in Figure 4.[20] Methyl Red molecules from both strands were stacked axially in an antiparallel manner between the base-pairs of adjacent G^3–C^{14} and C^6–G^{11}, as we designed.

Spectroscopic properties of the Methyl Red cluster: To investigate the effect of the clustering of Methyl Reds on spectroscopic behavior, UV/Vis and CD spectra were measured initially with the **NMR-D** duplex, in which stacking of the Methyl Reds was evidenced from the NMR analyses. At 60 °C, at which no duplex was formed, the UV/Vis spectra of self-complementary **NMR-D** was rather broad, with an absorption maximum at 477 nm, and CD was almost nil (see dotted lines in Figure 5). However, as the temperature was lowered to below the melting temperature (T_m), the absorption maximum shifted to shorter wavelengths (λ_{max} at 470 nm), and the spectrum became slightly narrower (see solid lines in Figure 5). Concurrently, a positive couplet was strongly induced at around 450 nm. This spectroscopic behavior is characteristic of the H-aggregation of dye mole-

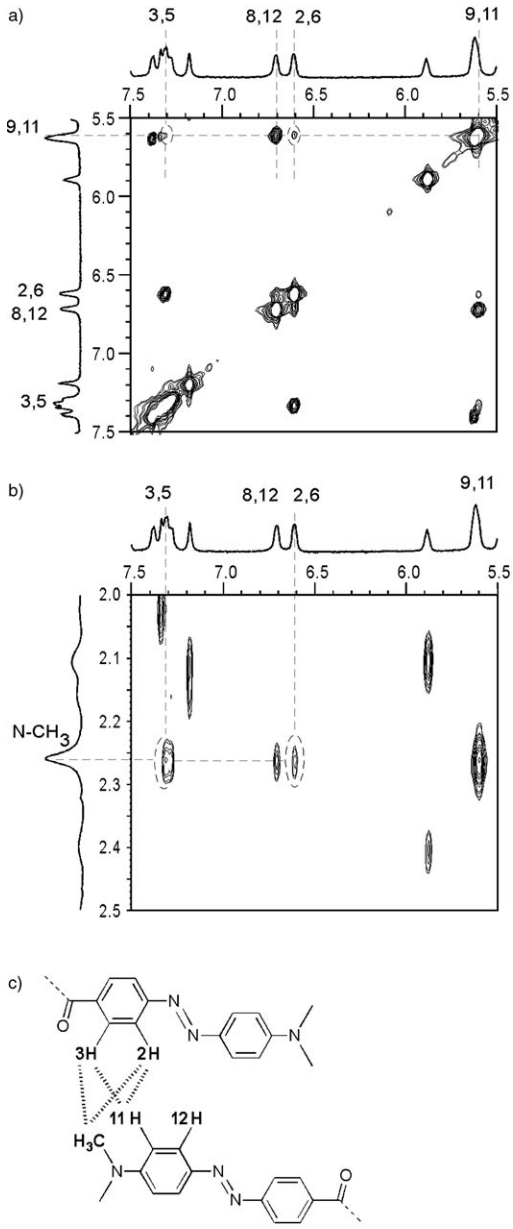

Figure 3. Two-dimensional NOESY spectra (mixing time = 100 ms) between the regions of 5.5–7.5 ppm (a) and between 5.5–7.5 ppm and 2.0–2.5 ppm (b) for the **NMR-D** duplex in D_2O at 280 K, pH 7.0 (10 mM phosphate buffer), in the presence of 200 mM NaCl. The NOE signals surrounded by circles demonstrate antiparallel stacking of Methyl Reds, which is illustrated in (c).

cules.[13] Thus, the dimerization of Methyl Reds from two complementary strands composed of **D** and **S** residues resulted in H-aggregation (H-band), as demonstrated by the results of NMR and UV/Vis spectroscopy.[13]

The effect of the number of clustered Methyl Reds on UV/Vis and CD spectra was systematically investigated by using a series of **DS*n*A/DS*n*B** duplexes at 0 °C, at which temperature the duplex was stably formed. As shown in Figure 6a, an increase in the number of Methyl Reds caused a larger hypsochromic shift: UV/Vis spectra of **DS1A/DS1B**, **DS2A/DS2B**, and **DS3A/DS3B** duplexes involving two, four, and six Methyl Reds, respectively, showed λ_{max} at 473, 451, and 445 nm, respectively. The intensity of induced CD (ICD) with a positive couplet also increased as the cluster size grew (Figure 6b), especially as the number of clusters increased from two (**DS1A/DS1B**) to four (**DS2A/DS2B**). Natural oligonucleotides in the **DS*n*A/DS*n*B** duplex formed a right-handed B-type helix, suggested by the symmetrical positive couplet observed at around 260 nm (see Figure S4 of the Supporting Information). This tendency is consistent with the molecular exciton theory for H-aggregation, as proposed by Kasha, which predicts that a larger hypsochromic shift is induced as the aggregation number increases.[21] Thus, the interstrand clustering of Methyl Reds demonstrated by the present design produces H-aggregates. Notably, Methyl Reds in the single-stranded **DS*n*A** or **DS*n*B** ($n \geq 2$) were essentially isolated, due to their separation by **S** residues, and were not strongly coupled.[12] Therefore, the H-aggregated cluster could be reversibly converted to the monomeric state by elevating the temperature to above T_m: bathochromic shift was induced by the dissociation of the duplex, and concurrently, the ICD disappeared (see Figure S5).

Previously, we have synthesized Methyl Red clusters by introducing multiple Methyl Reds sequentially into single-stranded DNA, such as **D6** in Scheme 1b.[12a] The **D6** species, involving six Methyl Reds, showed large hypsochromicity: the absorption maximum appeared at 415 nm.[12,13] The present interstrand clustering of Methyl Reds in an antiparallel manner (**DS3A/DS3B**) also induced both hypsochromic shift and narrowing of the band. However, interestingly, the UV spectra of **D6** and **DS3A/DS3B** were entirely different from each other (see Figure S6).

Effect of chirality of the linker on the spectroscopic behavior and stability of the duplex: Clustering (H-aggregation) was also achieved by using Methyl Red moieties tethered on L-threoninol, as evidenced by distinct hypsochromicity upon hybridization. Absorption maxima of **LS2A/LS2B** and **LS3A/LS3B** duplexes appeared at 446 and 438 nm, respectively, which was 5–7 nm shorter than the corresponding H-aggregates from D-threoninol, as shown in Figure 7a and Table 1. Although chirality of the linker had little effect on the UV/Vis spectra, a significant difference was observed in the CD spectra, as shown in Figure 7b. Induced CDs of **LS2A/LS2B** and **LS3A/LS3B** were a fraction (about $^1/_6$) of those of the **DS2A/DS2B** and **DS3A/DS3B** duplexes (compare Figures 7b and 6b).

Chirality of the linker also affected the stability of the duplex, as summarized in Table 1. The melting temperature (T_m) of the **DS1A/DS1B** duplex was 47.1 °C, which was almost the same as that of **NA/NB** (47.7 °C), the corresponding native duplex. An increase in the number of clusters on D-threoninol did not destabilize the duplex, but raised the T_m: T_ms of **DS2A/DS2B** and **DS3A/DS3B** were 51.5 and 50.9 °C, respectively (see Figure S7 for the actual melting curves). However, the T_m values of the correspond-

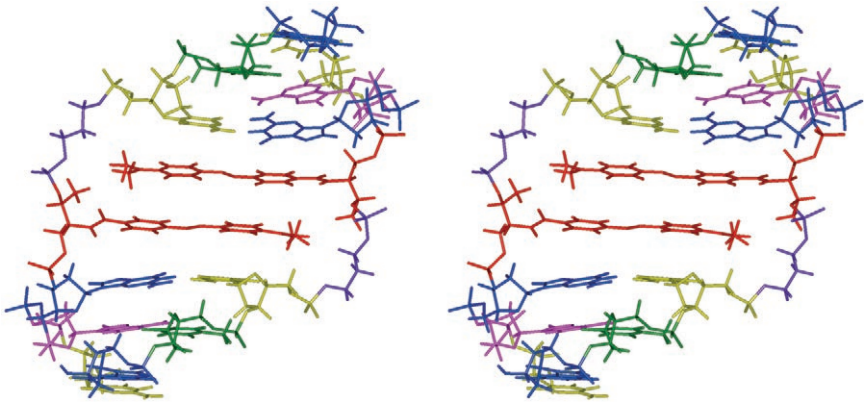

Figure 4. Minimized averaged total structure (stereoview) of **NMR-D** viewed from the side of the Methyl Red molecules. **X, S, A, T, G**, and **C** are colored red, purple, pink, green, blue, and yellow, respectively.

ing duplexes on L-threoninol were lower than those on the D-form. Especially for the **LS2A/LS2B** duplex, T_m was much lower than the native **NA/NB** duplex.

Discussion

Interstrand clustering of Methyl Red by hybridization: For the clustering of functional molecules, we use a tentative "base-pair" composed of a residue of a functional molecule on a threoninol linker (in this paper, **D** or **L** residue) and a 1,3-propanediol residue (**S** residue). As evidenced from the NMR analyses of the self-complementary **NMR-D** duplex, two Methyl Reds were axially stacked antiparallel to each other between the natural base-pairs, as depicted in Figure 4. The spectroscopic properties of a series of **DS*n*A/**

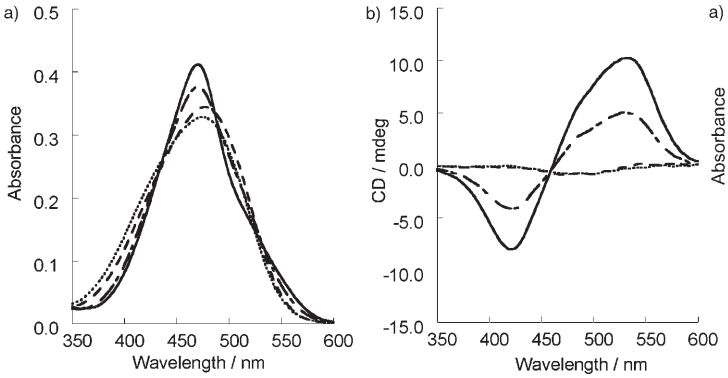

Figure 5. Change in spectroscopic behavior caused by the clustering of Methyl Reds in the **NMR-D** self-complementary duplex in the presence of 200 mM NaCl at pH 7.0 (10 mM phosphate buffer). a) UV/Vis spectra, b) CD spectra. Concentration of **NMR-D** was 10 μM. Melting temperature was determined as 26.0 °C from the change in absorbance at 260 nm as a function of temperature under the conditions employed: —— 0, –•–• 20, – – – 40, ••••• 60 °C.

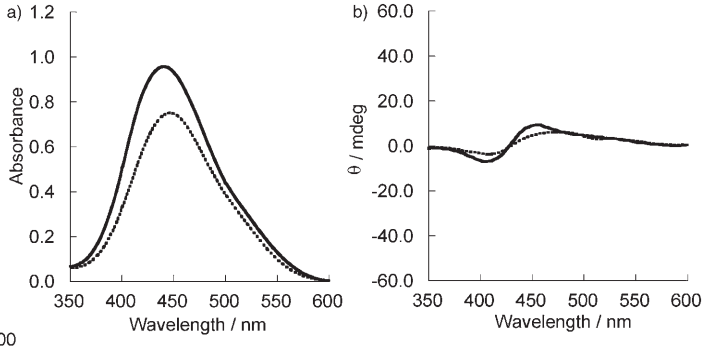

Figure 7. Effect of the number of clusters (cluster size) on spectroscopic behavior, obtained by using a series of **LS*n*A/LS*n*B** duplexes. a) UV/Vis spectra, b) CD spectra. Concentration of each conjugate was 5 μM. These spectra were measured at 0 °C in the presence of 100 mM NaCl at pH 7.0 (10 mM phosphate buffer). Note that the axes are on the same scale as those of Figure 6. ••••• **LS2A/LS2B**, —— **LS3A/LS3B**.

Table 1. Effect of the aggregation number and chirality of the linker on melting temperature (T_m) and absorption maximum.

Duplex	T_m [°C][a]	λ_{max} at 0 °C [nm][b]
DS1A/DS1B	47.1	473
DS2A/DS2B	51.5	451
DS3A/DS3B	50.9	445
LS2A/LS2B	43.5	446
LS3A/LS3B	48.5	438

[a] T_m was determined from the change in absorbance at 260 nm as a function of temperature (see Experimental Section for details). The T_m of the natural **NA/NB** duplex without **D** or **S** residues was 47.7 °C. [b] Both spectroscopic and T_m measurements were conducted at pH 7.0 (10 mM phosphate buffer) in the presence of 100 mM NaCl. The concentration of each strand was 5 μM.

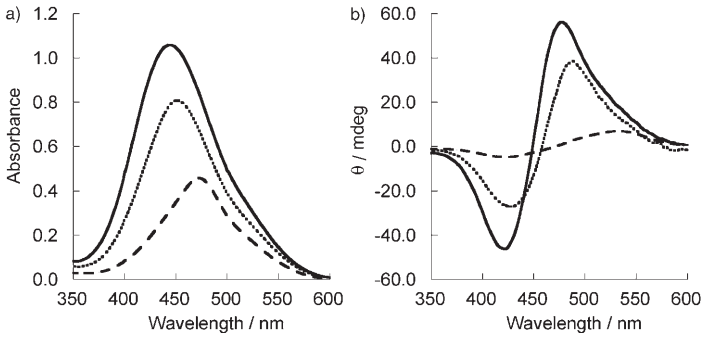

Figure 6. Effect of the number of clusters (cluster size) on spectroscopic behavior, obtained by using a series of **DS*n*A/DS*n*B** duplexes. a) UV/Vis spectra, b) CD spectra. Concentration of each conjugate was 5 μM. These spectra were measured at 0 °C in the presence of 100 mM NaCl at pH 7.0 (10 mM phosphate buffer). Both the melting temperature and λ_{max} of each duplex are summarized in Table 1. – – – **DS1A/DS1B**, ••••• **DS2A/DS2B**, —— **DS3A/DS3B**.

DS*n*B or **LS*n*A**/**LS*n*B** duplexes also demonstrate the stacking of incorporated Methyl Reds, substantiating the validity of our design for the clustering of functional molecules. Although the pair of **D** and **S** residues does not involve any complementary hydrogen bonding, the DNA conjugates form a sufficiently stable duplex. The introduction of non-natural residues often significantly destabilizes the duplex, relative to the corresponding natural duplex. However, as shown in Table 1, these non-natural residues did not destabilize the duplex, but rather slightly stabilized it by increasing the number of Methyl Reds. Because Methyl Reds from each strand were alternately stacked beside each other, stacking interactions among the dye molecules compensated for any destabilization of the duplex that should be caused by the presence of non-natural residues. Nevertheless, the self-assembling force inherent to Methyl Red molecules is not appreciably strong, as seen by the absence of clustering for **LSLSLS**, which had no natural DNA tags at either termini (data not shown). Thus, clustering of Methyl Reds was associated with the hybridization force of natural DNA.

Spectroscopic behavior of clustering of Methyl Reds: Because hybridization induced distinct hypsochromicity of Methyl Red, it can be concluded that the present cluster is an H-aggregate.[13] Larger hypsochromicity by the multiplication of dye molecules is also characteristic of H-aggregation. However, the UV spectrum of this cluster was entirely different from that of the cluster in which Methyl Reds were incorporated into the single strand, as previously reported (such as **D6**, see Figure S6). The absorption maximum of **DS3A**/**DS3B** involving six Methyl Reds appeared at 445 nm, and **D6** with the same six dye molecules showed λ_{max} at 415 nm. Furthermore, a significant decrease in the absorbance at λ_{max} (hypochromicity) occurred for the cluster in **D6**. These differences are based on the mutual orientation of the static molecular dipole moments. Because the dye molecules in **D6** are stacked parallel to each other, each dipole moment of the dye is identical and thus, strong interaction is possible. This strong interaction also induces strong hypochromicity. In the case of **DS3A**/**DS3B**, because the dye molecules are stacked in an antiparallel manner, **DS3A**/**DS3B** shows small hypsochromicity and hypochromicity, due to the weak interaction. Thus, spectroscopic behavior is controllable by cluster design.

Effect of the chirality of the linker on the structure of the cluster: The strong ICD with a positive couplet resulting from the hybridization of **DS*n*A**/**DS*n*B** indicates that Methyl Reds were stacked by forming a right-handed helix if D-threoninol was used as a linker. This ICD was enhanced especially as the number of stacked dye molecules increased from two (**DS1A**/**DS1B**) to four (**DS2A**/**DS2B**). This would be attributed to the difference of the winding angle of these clusters. The orientation of the dye molecules in **DS1A**/**DS1B** is expected to give almost the same stacking structure as the **NMR-D** duplex, because both the UV and CD spectra were very similar (compare solid lines in Figure 5 with broken lines in Figure 6). From the NOESY analysis of the **NMR-D** duplex, winding of the dye molecules in **NMR-D** was small (see Figure 4), and thus, the ICD was not so large. However, four dye molecules in the **DS2A**/**DS2B** duplex would have a much larger winding angle, due to the intrinsic clockwise winding property of D-threoninol, resulting in a larger ICD.

In contrast, **LS*n*A**/**LS*n*B** duplexes showed much lower ICD, demonstrating that the clockwise winding of Methyl Reds on L-threoninol is weak. This helical property is based on the nature of threoninol. Molecules on D-threoninol tend to wind clockwise, whereas those on L-threoninol wind counterclockwise.[12a,22] Because winding of Methyl Reds on D-threoninol corresponds to the natural DNA duplex, clusters in the **DS*n*A**/**DS*n*B** duplex easily formed a right-handed helix. In contrast, Methyl Reds on L-threoninol prefer counterclockwise winding that conflicts with the clockwise winding of natural base-pairs on the dye clusters. Consequently, the right-handed helix of the natural DNA portion interfered with the intrinsic counterclockwise helicity of L-threoninol, and thus, winding of Methyl Reds became much weaker. The difference in λ_{max} between **DS*n*A**/**DS*n*B** and **LS*n*A**/**LS*n*B**, although small, probably reflects this helical structure. These results suggest that the orientation of each dye molecule in the cluster is controllable by the linker.

The helical properties also affected the thermal stability of the duplexes. For the **DS*n*A**/**DS*n*B** duplex, because the clockwise winding of the dye molecules on D-threoninol did not interfere with the right-handed helix of natural DNA, T_m was only slightly increased by the accumulation of the dye. In contrast, the counterclockwise winding property of the dye molecules on L-threoninol interfered with the winding of the natural duplex and, accordingly, T_m was lowered in the case of a series of **LS*n*A**/**LS*n*B** duplexes.

Conclusion

1) Clustering of Methyl Reds was attained by hybridization of two complementary DNA–dye conjugates, each involving a Methyl Red moiety on a threoninol linker and a 1,3-propanediol spacer arranged alternately in the middle of the DNA sequence. A stacked structure was evidenced from the NMR analyses.
2) Antiparallel clustering of Methyl Reds induced a distinct hypsochromic shift, and the degree of hypsochromicity increased as the number of dye molecules increased. This spectroscopic behavior is characteristic of the H-aggregates of the dyes.
3) Chirality of threoninol affected both the ICD and the stability of the duplex, due to its winding properties.

By using this method, a hetero cluster of two different and alternating dyes is also easily prepared.[23] Because some optical properties, such as nonlinear optical activity,

are exhibited only by clustered dyes,[24] the present dye cluster may also be applicable as a new DNA probe of high sensitivity.

Experimental Section

Materials: All the conventional phosphoramidite monomers, CPG columns, the reagents for DNA synthesis, and Poly-Pak cartridges were purchased from GLEN RESEARCH. Other reagents for the synthesis of the phosphoramidite monomers were purchased from Tokyo Kasei, and Aldrich.

Synthesis of the modified DNA involving Methyl Red: All the modified DNAs were synthesized by using an automated DNA synthesizer, with phosphoramidite monomers corresponding to **D** and **L** residues, which were synthesized according to a previous report,[12a] as well as other conventional monomers. The coupling efficiency of the monomer corresponding to the **D** or **L** residue was as high as that of a conventional monomer, as judged from the coloration of released trityl cation. After the recommended work-up, the DNAs were purified by using reversed-phase HPLC.

MALDI-TOF MS: *m*/*z* calcd for **DS1A** $[M-H^+]$: 4199; found: 4200; *m*/*z* calcd for **DS1B** $[M-H^+]$: 4199; found: 4201; *m*/*z* calcd for **DS2A** $[M-H^+]$: 4755; found: 4756; *m*/*z* calcd for **DS2B** $[M-H^+]$: 4755; found: 4757; *m*/*z* calcd for **DS3A** $[M-H^+]$: 5311; found: 5311; *m*/*z* calcd for **DS3B** $[M-H^+]$: 5311; found: 5311; *m*/*z* calcd for **NMR-D** $[M-H^+]$: 2347; found: 2348; *m*/*z* calcd for **LS2A** $[M-H^+]$: 4755; found: 4757; *m*/*z* calcd for **LS2B** $[M-H^+]$: 4755; found: 4757; *m*/*z* calcd for **LS3A** $[M-H^+]$: 5311; found: 5312; *m*/*z* calcd for **LS3B** $[M-H^+]$: 5311; found: 5313.

Spectroscopic measurements: The UV/Vis and CD spectra were measured by using a JASCO model V-530 and a JASCO model J-730, respectively, with a 10 mm quartz cell. Both instruments were equipped with programmed temperature-controllers. Conditions of the sample solutions were as follows (unless otherwise noted): [NaCl] = 100 mM, pH 7.0 (10 mM phosphate buffer), [DNA] = 5 μM.

Measurement of melting temperature: The melting curves of the duplexes were obtained by using the above apparatus to measure the change in absorbance at 260 nm versus temperature. The melting temperature (T_m) was determined from the maximum in the first derivative of the melting curve. Both the heating and cooling curves were obtained, and the T_m values measured from them coincided with each other to within 2.0 °C. The T_m values presented here are an average of 2–4 independent experiments. The error of the T_m values is ±1.0 °C.

NMR measurements: NMR samples were prepared by dissolving three-times-lyophilized DNAs (modified and complementary DNA) in a H_2O/D_2O 9:1 solution containing 10 mM sodium phosphate (pH 7.0) to give a duplex concentration of 1.0 mM. NaCl was added to a total sodium concentration of 200 mM. After NMR measurement in H_2O/D_2O, the samples were lyophilized again and dissolved in a D_2O solution.

NMR spectra were measured by using an Avance-600 spectrometer (Bruker) at a probe temperature of 280 K. Two-dimensional NOESY (mixing time of 150 ms) spectra[25] in H_2O/D_2O 9:1 were recorded by using the States-TPPI method[26] and 3–9–19 WATERGATE pulse sequence for water suppression. FIDs (128 scans of each) of 2 K data points in the t_2 domain were collected for 512 data points in the t_1 domain. Prior to Fourier transformation, the spectra were zero-filled to give final 2 K × 1 K data points after apodization with a π/2-shifted squared sinebell function. Two-dimensional NOESY (mixing times of 100 and 200 ms), TOCSY (mixing time of 60 ms),[27] and DQF-COSY spectra[28] in D_2O were recorded by using the States-TPPI method without suppression of the H_2O signal. Free induction decay signals (FIDs) of the 2 K data points in the t_2 domain were collected for the 512 data points in the t_1 domain. The number of scans for NOESY, TOCSY, and DQF-COSY in D_2O was 96. Prior to Fourier transformation, Gaussian window functions were applied to both dimensions.

Structure restraints and calculation: NOE intensities obtained from two-dimensional NOESY spectra in D_2O with a mixing time of 100 ms were interpreted as interactions of very strong (0–3), strong (0–4), medium (0–5), or weak (0–6 Å). A few other interproton distances were obtained from the NOESY spectra in H_2O with a mixing time of 150 ms. By using cross-peaks corresponding to the fixed 2.4 Å deoxycytidine H5–H6 distance as internal references, interproton distances corresponding to each of the cross-peaks were calculated by using the program Felix (Molecular Simulation). For the distance restraints, upper and lower limits were defined as +1.5 and −1 Å calculated distances, respectively. Hydrogen-bonding restraints from Watson-Crick base-pairs were introduced as distance restraints between the proton and heavy atom (1.8–2.5 Å). Structural restraints are summarized in Table S1 of the Supporting Information. Existence of hydrogen bonding for base-pairs was judged from a significant downfield shift of the imino-proton resonance and a slow rate of exchange with the solvent. For the residues at the ends of each strand (C^1, C^8, G^9, and G^{16}), restraints on the typical B-form DNA structure were introduced on the assumption that the **D** and **S** residue would not influence the structure of the ends of the DNA strands.

A set of 100 structures was calculated by using a simulated annealing protocol with the InsightII/Discover package (Molecular Simulation). The AMBER was used as the force field. A total of 256 NOE distance restraints and 64 dihedral restraints were used for the calculation. The force constants were 50 kcal mol^{-1} Å^{-2} for distance restraints and 50 kcal mol^{-1} rad^{-2} for dihedral restraints. The atomic coordinates were randomized prior to the calculation. Distance and dihedral restraints were gradually scaled to full value during 15 ps of molecular dynamics at 1000 K, while maintaining low value for interatomic repulsion, which was subsequently increased to full value during another 21 ps of dynamics. An additional 5 ps of dynamics was performed at 1000 K and the temperature was gradually scaled to 300 K during 10 ps. A final minimization step was performed, which included a Lennard–Jones potential and no electrostatic terms. The ten final structures with the lowest total and restraint violation energies were chosen.

Acknowledgements

This work was financially supported by Precursory Research for Embryonic Science and Technology (PRESTO), Japan Science and Technology Agency (JST). Partial support by The Mitsubishi Foundation (for H.A.) and a Grant-in-Aid for Scientific Research from the Ministry of Education, Science, and Culture, Japan is also acknowledged. This work was also supported by, in part, a Grant-in-Aid for High Technology Research from the Ministry of Education, Science, Sports, and Culture, Japan.

[1] R. Vallée, P. Damman, M. Dosière, E. Toussaere, J. Zyss, *J. Am. Chem. Soc.* **2000**, *122*, 6701–6709.
[2] S. Shukla, S. Zeal, *Nanostruct. Mater.* **1999**, *11*, 1181–1193.
[3] A. N. Shipway, E. Katz, I. Willner, *ChemPhysChem* **2000**, *1*, 18–52.
[4] I. Place, J. Perlstein, T. L. Penner, D. G. Whitten, *Langmuir* **2000**, *16*, 9042–9048.
[5] a) M. Wang, G. L. Silvia, B. A. Armitage, *J. Am. Chem. Soc.* **2000**, *122*, 9977–9986; b) J. L. Seifert, R. E. Connor, S. A. Kushon, M. Wang, B. A. Armitage, *J. Am. Chem. Soc.* **1999**, *121*, 2987–2995.
[6] a) E. T. Kool, *Chem. Rev.* **1997**, *97*, 1473–1488; b) E. T. Kool, *Acc. Chem. Res.* **2002**, *35*, 936–943.
[7] a) K. Tanaka, A. Tengeiji, T. Kato, N. Toyama, M. Shionoya, *Science* **2003**, *299*, 1212–1213; b) J. Gao, C. Strässler, D. Tahmassebi, E. T. Kool, *J. Am. Chem. Soc.* **2002**, *124*, 11590–11591.
[8] Y. Ito, E. Fukusaki, *J. Mol. Catal. B: Enzym.* **2004**, *28*, 155–166.
[9] B. Yurke, A. J. Turberfield, A. P. Mills, F. C. Simmel, Jr., J. L. Neumann, *Nature* **2000**, *406*, 605–608.
[10] a) L. M. Adleman, *Science* **1994**, *266*, 1021–1024; b) K. Sakamoto, H. Gouzu, K. Komiya, D. Kiga, S. Yokoyama, T. Yokomori, M. Hagiya, *Science* **2000**, *288*, 1223–1226.

[11] B. Giese, *Curr. Opin. Chem. Biol.* **2002**, *6*, 612–618.
[12] a) H. Asanuma, K. Shirasuka, T. Takarada, H. Kashida, M. Komiyama, *J. Am. Chem. Soc.* **2003**, *125*, 2217–2223; b) H. Asanuma, K. Shirasuka, M. Komiyama, *Chem. Lett.* **2002**, 490–491.
[13] Generally, hypsochromicity without distinct narrowing is called the H-band, and the corresponding cluster is an H-aggregate. But if distinct narrowing as well as large hypsochromicity is observed, the cluster is called specifically an H*-aggregate. See Figure S1 of the Supporting Information.
[14] Azo dyes are also convenient, as they are sufficiently stable during DNA synthesis, which requires highly basic and acidic conditions. Furthermore, positive charge can be easily introduced by changing the pH of the solution. However, the optical properties of these dyes are not distinctive enough to enable a detailed discussion of their spectroscopic behavior . For this purpose, cyanines or porphyrins would be more appropriate.
[15] C. Brotchi, C. J. Leumann, *Angew. Chem.* **2003**, *115*, 1694–1697; *Angew. Chem. Int. Ed.* **2003**, *42*, 1655–1658; .
[16] Without the **S** residue, H*-aggregates are formed in the single-stranded state, as reported previously. See reference [12a].
[17] Measurement of T_m was performed in the presence of 200 mM NaCl at pH 7.0 (10 mM phosphate buffer). Concentration of **NMR-D** was 5 μM. These solution conditions were identical to those of the NMR measurements, except for the concentration of **NMR-D**.
[18] As the temperature was raised, the imino-proton signal of terminal G^{16} was further broadened, and concurrently shifted to a higher magnetic field compared with other signals.
[19] Other intramolecular NOE signals, such as between H9 (H11) and H8 (H12), remained at 60 °C. See Figure S2 of the Supporting Information.
[20] Superimposition of the ten final converged structures is presented in Figure S3 of the Supporting Information.
[21] E. G. McRae, M. Kasha, *J. Chem. Phys.* **1958**, *28*, 721–722.
[22] X. Liang, H. Asanuma, H. Kashida, A. Takasu, T. Sakamoto, G. Kawai, M. Komiyama, *J. Am. Chem. Soc.* **2003**, *125*, 16408–16415.
[23] H. Kashida, H. Asanuma, M. Komiyama, *Angew. Chem.* **2004**, *116*, 6684–6687; *Angew. Chem. Int. Ed.* **2004**, *43*, 6522–6525; .
[24] V. V. Shelkovnikov, R. V. Markov, A. I. Plekhanov, A. E. Simanchuk, Z. M. Ivanova, *High Energy Chem.* **2002**, *36*, 260–264.
[25] J. Jeener, B. H. Meier, P. Bachmann, R. R. Ernst, *J. Chem. Phys.* **1979**, *71*, 4546–4553.
[26] D. Marion, M. Ikura, R. Tschudin, A. Bax, *J. Magn. Reson.* **1989**, *85*, 393–399.
[27] C. Griesinger, G. Otting, K. Wüthrich, R. Freeman, *J. Am. Chem. Soc.* **1988**, *110*, 7870–7872.
[28] A. J. Shaka, R. Freeman, *J. Magn. Reson.* **1983**, *51*, 169–173.

Received: January 31, 2005
Revised: June 1, 2005
Published online: September 15, 2005

